Applied Physics Letters

Localized strain relaxation effect on gamma irradiated AlGaN/GaN high electron mobility transistors

Cite as: Appl. Phys. Lett. **121**, 233502 (2022); https://doi.org/10.1063/5.0125481
Submitted: 12 September 2022 • Accepted: 16 November 2022 • Published Online: 05 December 2022

Nahid Sultan Al-Mamun, Sergei Stepanoff, Aman Haque, et al.

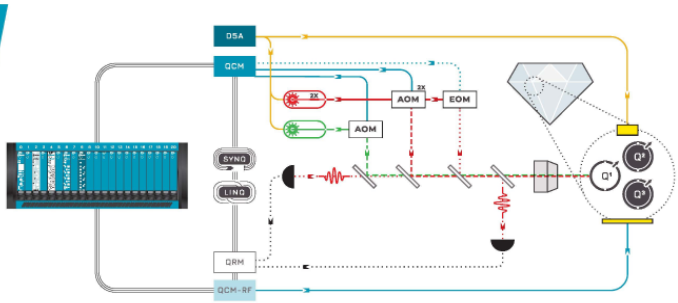

Applied Physics Letters ARTICLE scitation.org/journal/apl

Localized strain relaxation effect on gamma irradiated AlGaN/GaN high electron mobility transistors

Cite as: Appl. Phys. Lett. **121**, 233502 (2022); doi: 10.1063/5.0125481
Submitted: 12 September 2022 · Accepted: 16 November 2022 ·
Published Online: 5 December 2022

Nahid Sultan Al-Mamun,[1] Sergei Stepanoff,[2] Aman Haque,[1,a)] Douglas E. Wolfe,[2] Fan Ren,[3] and Stephen Pearton[4]

AFFILIATIONS

[1]Department of Mechanical Engineering, Penn State University, University Park, Pennsylvania 16802, USA
[2]Department of Materials Science and Engineering, Penn State University, University Park, Pennsylvania 16802, USA
[3]Department of Chemical Engineering, University of Florida, Gainesville, Florida 32611, USA
[4]Department of Material Science and Engineering, University of Florida, Gainesville, Florida 32611, USA

[a)]Author to whom correspondence should be addressed: mah37@psu.edu

ABSTRACT

Strain localization in microelectronic devices commonly arises from device geometry, materials, and fabrication processing. In this study, we controllably relieve the local strain field of AlGaN/GaN HEMTs by milling micro-trenches underneath the channel and compare the device performance as a function of the relieved strain as well as radiation dosage. Micro-Raman results suggest that the trenches locally relax the strain in device layers, decreasing the 2DEG density and mobility. Intriguingly, such strain relaxation is shown to minimize the radiation damage, measured after 10 Mrads of ^{60}Co-gamma exposure. For example, a 6-trench device showed only ∼8% and ∼6% decrease in saturation drain current and maximum transconductance, respectively, compared to corresponding values of ∼15% and ∼30% in a no-trench device. Negative and positive threshold voltage shifts are observed in 6-trench and no-trench devices, respectively, after gamma radiation. We hypothesize that the extent of gamma radiation damage depends on the strain level in the devices. Thus, even though milling a trench decreases 2DEG mobility, such decrease under gamma radiation is far less in a 6-trench device (∼1.5%) compared to a no-trench device (∼20%) with higher built-in strain.

Gallium nitride (GaN) is a wide bandgap material with high critical electric field, electron mobility, and thermal conductivity, enabling high power and high speed electronic devices.[1,2] It is attractive for radiation environment as well, because GaN has lower rate of defect generation upon irradiation than Si due to its higher threshold energy for atomic displacement.[3,4] The performance of AlGaN/GaN HEMTs upon irradiation has mostly been studied as a function of radiation type, dose, and energy as well as initial carrier density, impurity content, and dislocation density of the device.[5] The response to gamma radiation of GaN HEMTs have been reported with contradictory results. Some studies[6–10] reported improvement of device performance, including higher saturation drain current, carrier concentration, and mobility due to partial relaxation of strain in AlGaN/GaN heterostructure and uniform redistribution of defects and traps after gamma radiation. Other studies[11–18] reported degraded transport properties of GaN HEMTs as a result of gamma radiation induced additional defects and traps generation. Both positive[14,18–20] and negative[6,7,19] shift of threshold voltage have been reported upon gamma radiation. In addition to the accumulated radiation dose and dose rate, the structural differences, such as presence of passivation layer, materials in the Ohmic and gate contacts, gate length, and width, are reported to play an important role in the discrepancy of gamma radiation response of GaN HEMTs.[13,20–22]

Even though the influence of mechanical strain is extensively studied in the literature, how it affects the post irradiation performance is less understood. In particular, nano or microscale strain localizations are yet to be studied. Existing studies involve only uniform strain through using different substrate materials,[23,24] cantilever,[25] 3 and 4-point bending,[26,27] and substrate removal techniques.[28,29] Spatial mapping of strain is very difficult, and the global average can be negligible, even with very high magnitudes of tensile and compressive localized strain. The core theme of this study is that highly localized strain can

act as 'mechanical hotspots' to facilitate nucleation of defects and traps under radiation; a hypothesis that cannot be properly elucidated with global strain. Residual strain in the AlGaN/GaN HEMT originates during fabrication due to the heteroepitaxial growth of lattice and thermal expansion coefficient mismatched materials on foreign substrates.[23,30,31] Depending on the substrate material and growth process, the residual strain in the GaN layer could be tensile or compressive, whereas the residual strain in the AlGaN layer is mostly tensile.[5,32] Strain can influence the mobility of 2DEG electrons by changing the band structure and trap energy, which can impact the performance and reliability of GaN HEMTs.[33] Excessive residual strain in the AlGaN layer can cause strain relaxation during operation, nucleating defects which act as trapping centers for electrons, and reduces the carrier concentration and mobility of the device.[34,35] There is very little or no understanding of the impact of preexisting strain condition and the spatial distribution of strain within the GaN HEMTs under radiation. Therefore, in this research, we investigate the effect of the preexisting strain condition through localized strain relaxation on the performance of AlGaN/GaN HEMTs after gamma radiation.

We adopted the strategy of the localized strain relief by milling micro-trenches under the channel, a technique commonly used to measure residual stress.[36] Local strain relief was achieved on the commercially available depletion mode AlGaN/GaN HEMTs (CGHV60008D, Wolfspeed®) by milling a 70 μm deep and 20×30 μm2 size micro-trenches. All trenches were systematically fabricated at the half width of the channel. Figure 1 schematically shows the pristine and 1, 3, and 6-trench devices that were exposed to cobalt-60 gamma (^{60}Co-γ) radiation of accumulated dose of 10 Mrads at a dose rate of 180 krads/h at room temperature. The strain in the GaN layer before and after gamma irradiation were mapped by micro-Raman spectroscopy with 2 and 0.5 μm step intervals along and across the device channel, respectively. Further details are given in Ref. 37, where we observed strong influence of a single trench on the overall 2DEG mobility.

High-resolution micro-Raman spectra were obtained at room temperature on the AlGaN/GaN channel in order to determine the biaxial residual stress (σ_{xx}) and in-plane strain (ε_{xx}) of the devices. The strain maps across the channel in pristine and micro-trenched devices are shown in Fig. 2(a). Relaxation of residual tensile stress and strain was observed in the micro-trenched devices in the vicinity of the trench. Figure 2(a) represents trends for the 3 and 6-trench devices as well, more micro-trenches resulting in higher strain relaxation. The corresponding strain maps after gamma irradiation with 10 Mrads are shown in Fig. 2(b). All devices showed "U" shaped distribution of strain across the channel, except for source to gate region of micro-trenched device, suggesting higher strain at the edges of the source, gate, and drain contacts. The deviation of the micro-trenched device could be associated with the redistribution of strain as a result of creating trench under the channel. The FWHM of E_2 (high) peak was found to broaden from 2.39 ± 0.10 to 2.65 ± 0.14 and 2.45 ± 0.11 to $2.64 \pm 0.12\,\mathrm{cm}^{-1}$ for pristine and micro-trenched channels, respectively, after gamma radiation. This suggests the increase in the defects and traps, which might lower 2DEG mobility in GaN HEMTs.[38]

The output characteristics (I_{ds}–V_{ds}) of the pristine and micro-trenched devices are shown in Fig. 3(a). The saturation drain current of micro-trenched devices are found to be smaller compared to the pristine device. The increase in the trench numbers on the substrate of the device results in higher reduction in the saturation drain current, which could be associated with the relaxation of higher strain in the conductive channel and/or change in heat dissipation capacity as a result of substrate micro-trenching. However, if the increase in self-heating on the substrate micro-trench device is the reason for lower saturation drain current, then the saturation drain current difference between the micro-trenched and the pristine devices should have increased with the increase in the gate bias. However, such trait has not been observed in the I_{ds}–V_{ds} curves. In addition, the total substrate area of the micro-trench devices was reduced by only ~0.1%–1%

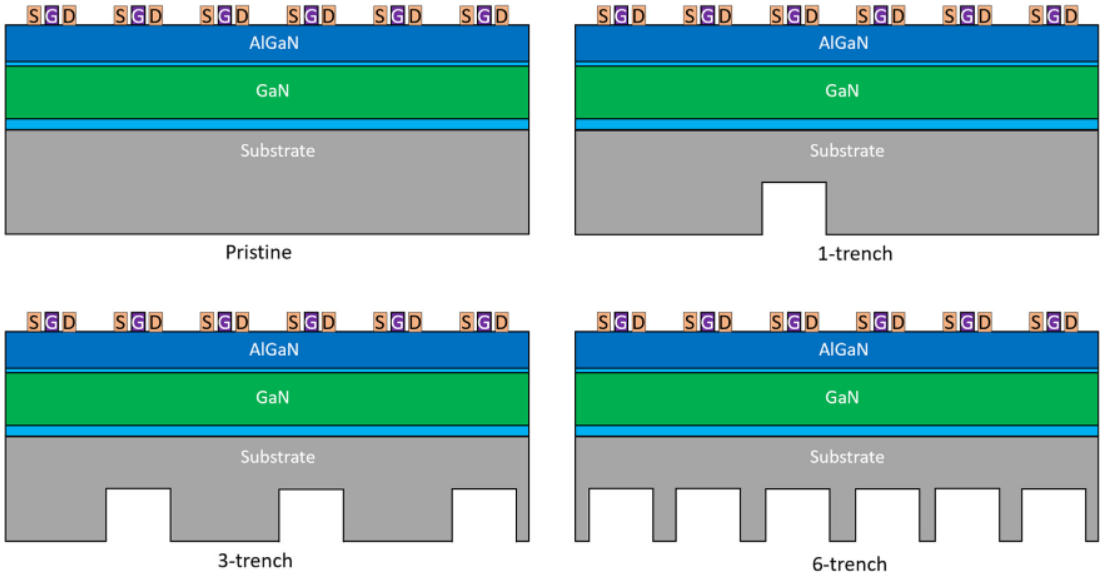

FIG. 1. Cross-sectional schematic (not up to scale) of pristine and micro-trenched devices along the plane of micro-trench.

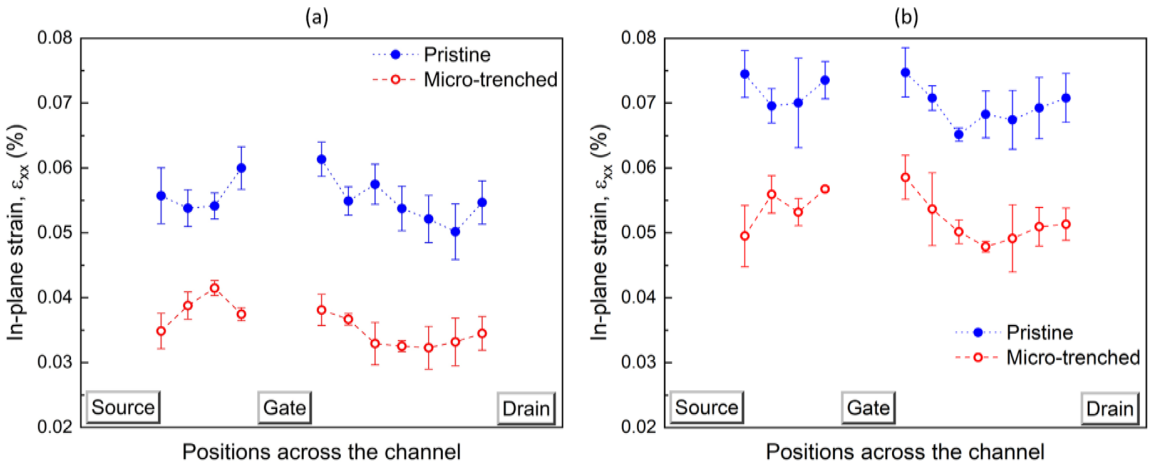

FIG. 2. In-plane residual strain distribution across the pristine and micro-trenched channel (1-trench device): (a) before gamma radiation and (b) after gamma radiation.

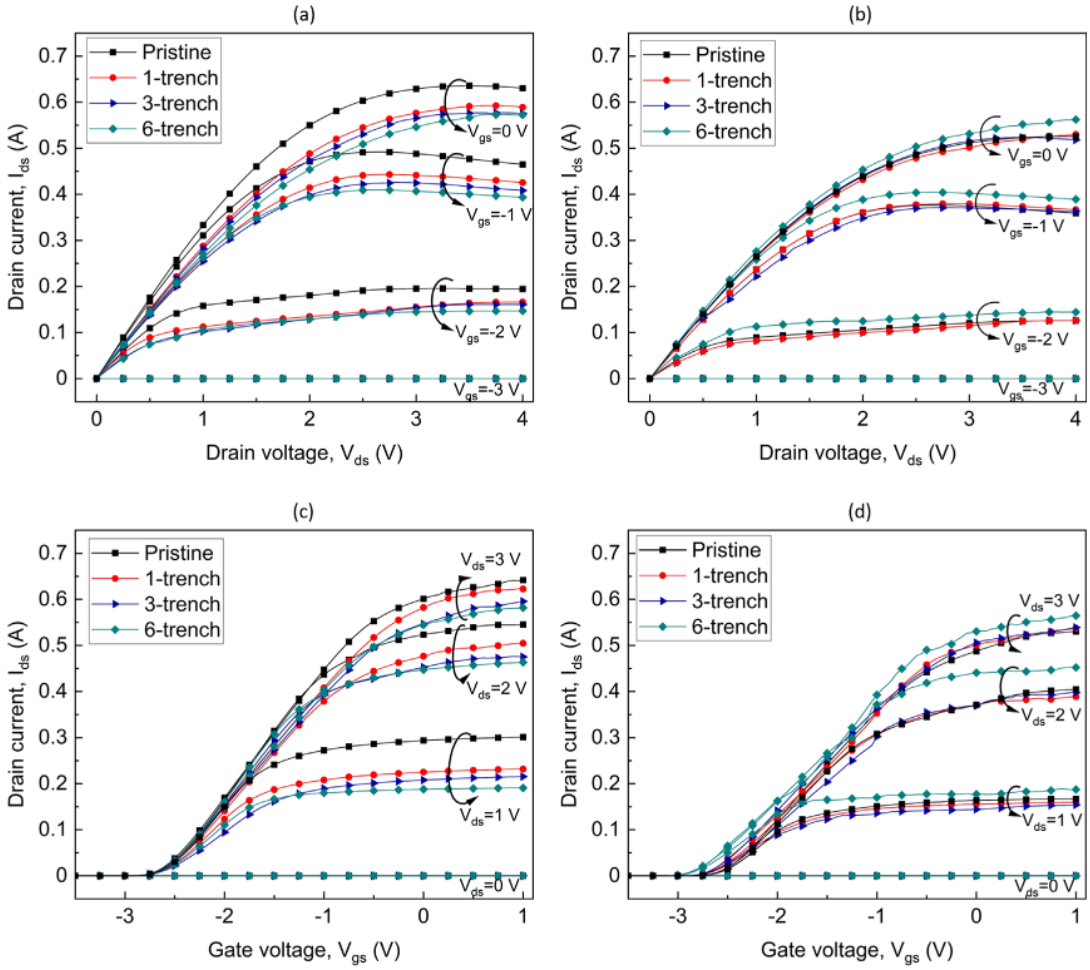

FIG. 3. DC characteristics of pristine and micro-trenched devices: (a) output curves (I_{ds}–V_{ds}) before gamma radiation, (b) output curves (I_{ds}–V_{ds}) after gamma radiation, (c) transfer curves (I_{ds}–V_{gs}) before gamma radiation, and (d) transfer curves (I_{ds}–V_{gs}) after gamma radiation.

compared to the pristine device. Such small reduction in the total substrate area can be assumed to be insignificant for the SiC substrate, which has good thermal conductivity (420 W/m K), to alter the heat dissipation capacity significantly. Therefore, we speculate that the change in the strain status of the micro-trenched devices is the dominant factor to contribute to the reduced saturation drain current.

The impact of gamma radiation on the output characteristics of devices with different strain conditions are shown in Fig. 3(b). Exposure to 10 Mrads of gamma irradiation caused significant reduction in the saturation drain current of all devices. Intriguingly, the saturation drain current of the 6-trench device was found to be higher compared to other devices after gamma radiation. The transfer curves of the GaN HEMTs before and after gamma irradiation are shown in Figs. 3(c) and 3(d), respectively. Before gamma irradiation, no difference in the threshold voltage (V_{th}) was observed among pristine and micro-trenched devices. After gamma irradiation, all devices exhibited a positive threshold voltage shift except the 6-trench device, where a negative threshold voltage shift was observed. At higher gamma radiation dose, the nitrogen vacancies produce acceptor like deep trap states, which increases the activation energy for carrier recombination.[12,14,15] As a result, a decrease in electron concentration in 2DEG channel after gamma radiation can be observed leading to reduction in the saturation drain current and positive shift of V_{th}, as reported in several studies at relatively higher dose of gamma radiation.[14,18–20] However, in the case of the 6-trecnh device, the negative shift of V_{th} after gamma radiation might be related to non-uniform strain distribution along every channel of the device, which might cause additional charge polarization by accumulating the positive charge in the strain localized regions or redistribution of charges around the strain localization after gamma radiation.[39,40]

Relative change in the important parameters, such as saturation drain currents ($I_{ds,sat}$), ON-resistance (R_{ON}), maximum transconductance (G_{max}), and threshold voltage (V_{th}) of the devices before and after gamma irradiation, have been reported in Table I. The gamma radiation induced degradation of the devices reduces with the increase in the number of trenches on the device. Such trend suggests that each trench only affects the device channel above that trench. After gamma radiation, the $I_{ds,sat}$ of the pristine device reduced by ∼15% at zero gate voltage (V_g), whereas in the case of the 6-trench device, the corresponding value reduced by ∼8%. The R_{ON} resistance of pristine and 6-trench device increased by ∼26% and ∼1%, respectively, at zero gate voltage after irradiation. The G_{max} of irradiated devices reduced by ∼30% and ∼6% at 1 V of drain voltage (V_d) for pristine and 6-trench device, respectively.

TABLE I. Gamma radiation induced relative change of drain saturation currents ($I_{ds,sat}$), ON-resistance (R_{ON}), maximum transconductance (G_{max}), and threshold voltage (V_{th}) of the devices.

Parameters	Pristine device	1-trench device	3-trench device	6-trench device
$\Delta I_{ds,sat}$ at $V_g = 0$ V (%)	−15.56	−13.10	−11.86	−7.92
ΔR_{ON} at $V_g = 0$ V (%)	+26.09	+19.39	+6.17	+0.58
ΔG_{max} at $V_d = 1$ V (%)	−30.47	−29.92	−14.28	−6.38
ΔV_{th} (V)	+0.09	+0.09	+0.07	−0.08

The gate leakage current of GaN HEMTs before and after gamma radiation is shown in Fig. 4. Before gamma radiation, the pristine device showed least leakage current and with the increase in the number of trenches in the device, leakage current increased. After gamma radiation, the leakage current of all devices increased. While the leakage currents of 1 and 3-trench devices were found to relatively higher, the corresponding values of pristine and 6-trench devices were comparable with least leakage current in the pristine device. Intriguingly, the 6-trench device showed the least radiation damage as the leakage current was very close to the pristine device.

Radiation induced reduction in the carrier concentration and mobility of the 2DEG channel was calculated from C–V measurements,[41–43] as shown in Figs. 5(a) and 5(b), respectively. The 2DEG carrier density was found to decrease slightly with the increase in trench numbers in the device before gamma radiation. After gamma radiation, the 2DEG carrier density of all devices decreased. However, no significant difference in the carrier density was monitored among the devices after gamma radiation. The electron mobilities at different gate biases are shown in Fig. 5(b). The micro-trenched devices showed smaller mobility compared to the pristine device with the increase in the trench number before gamma radiation. However, the mobility of the 6-trench device was found to be relatively higher at all gate voltages compared to other devices after gamma radiation. The product of 2DEG carrier density and mobility ($n_{2D}.\mu_n$) at zero gate voltage of the pristine device was found to be reduced by ∼20% after gamma radiation, whereas the corresponding value reduced only ∼1.5% in the case of the 6-trench device. The term $n_{2D}.\mu_n$ is inversely proportional to the resistivity of the 2DEG channel. Therefore, smaller decrease in the $n_{2D}.\mu_n$ value of the 6-trenched device compared to the pristine and other two devices resulted in gamma radiation induced lower degradation of DC transport properties of the 6-trench device, as reported in Table I.

The degradation of transport properties after gamma radiation is mostly dominated by the reduction of mobility of the devices, as the pronounced impact of gamma radiation on the mobility can be observed in Fig. 5(b). Before gamma radiation, lower mobility of

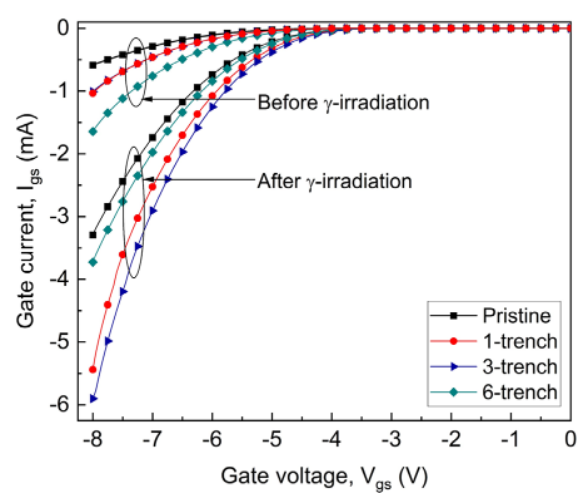

FIG. 4. Gate to source leakage currents of pristine and micro-trenched devices before and after gamma radiation.

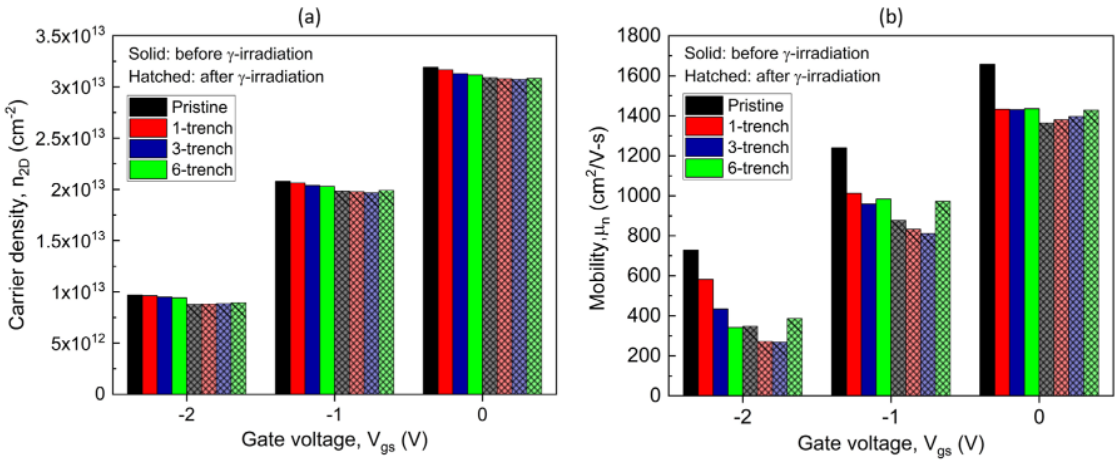

FIG. 5. (a) Carrier density and (b) mobility of 2DEG channel of pristine and micro-trenched devices before and after gamma radiation.

micro-trenched devices compared to the pristine device is mainly due to polarization coulomb field (PCF) scattering of electrons in the 2DEG channel resulted from the non-uniform strain distribution in the vicinity of strain released area along the channel.[39,41] As a result, with the increase in the number of trenches, the PCF scattering effect increases causing the least mobility in 6-trench device, which ultimately led to lowest saturation drain current and highest ON-resistance before gamma radiation. After gamma radiation, significant reduction in the electron mobility might be associated with the radiation induced defect formation as a result of increased strain value of the GaN layer. Higher strain in the GaN layer may cause strain relaxation in the AlGaN layer creating higher amount of defects and dislocations.[8,44,45] High defect density increases the population of deeper level traps and reduces the carrier diffusion length promoting scattering of electrons.[12] Therefore, gamma radiation induced 2DEG mobility degradation of the devices is dominated by higher dislocation and defect scattering phenomena of electrons.

We speculate that local strain relaxation in the vicinity of trenched location causes depletion of 2DEG reducing the current flow in the whole channel. Smaller residual tensile strain in the micro-trenched channel is expected to induce smaller operation related stress, i.e., electric field induced inverse piezoelectric stress and thermal stress along the channel[23] compared to the pristine channel. In the presence of higher number of defects and dislocations after gamma radiation, the strain relaxed channel experiences lower scattering effect compared to the strained channel due to reduced operational stress build-up along the channel, which resulted in relatively higher mobility of 6-trenched device after gamma radiation compared the pristine device leading to higher saturation drain current. However, the increase in the defect density such as vacancies and dislocations in the AlGaN and GaN layers after gamma radiation can assist tunneling of electrons through the barrier layer contributing to higher gate leakage current after gamma radiation,[16] as can be seen in Fig. 4. Negative gate bias reduces the tensile strain in the AlGaN layer during operation,[46,47] which resulted in relatively smaller gate leakage current in the pristine device compared to micro-trenched devices after gamma radiation. Relatively smaller gate leakage current of the 6-trench device compared to 1 and 3-trench devices is the result of higher strain relaxation induced lower electrical field stress under negative bias condition.

In summary, this study focused on the effects of the pre-existing localized strain on the gamma radiation damage susceptibility of AlGaN/GaN HEMTs. Localized relaxation of residual strain is shown to reduce the 2DEG sheet carrier density and electron mobility due to higher scattering events in the presence of the nonuniform strain distribution, which ultimately reduces the saturation drain current and transconductance of the device. The post-irradiation results demonstrate that relaxing the pre-existing strain can lower the radiation vulnerability, albeit at the cost of slightly lower saturation drain current. Although gamma radiation increases the density of defects and dislocations in the device layers, the strain relaxed channel experiences lower scattering of 2DEG electrons by defects, which might be associated with relatively smaller operation related stress build up along the channel compared to non-strain relaxed or pristine channel. As a result, the gamma radiation induced mobility degradation is minimized to some extent. However, localized strain relaxation could increase gate leakage current. Optimum condition to minimize radiation induced performance degradation and defect mitigation would be uniform strain relaxation of the device.

This work was funded by the Defense Threat Reduction Agency (DTRA) as part of the Interaction of Ionizing Radiation with Matter University Research Alliance (IIRM-URA) under Contract No. HDTRA1-20-2-0002. The work at UF was also supported by the NSF DMR 1856662 (James Edgar). The work at PSU was also supported by the NSF ECCS 2015795. The content of the information does not necessarily reflect the position or the policy of the federal government, and no official endorsement should be inferred.

AUTHOR DECLARATIONS

Conflict of Interest

The authors have no conflicts to disclose.

Author Contributions

Nahid Sultan Al-Mamun: Conceptualization (equal); Data curation (equal); Formal analysis (equal); Investigation (equal); Methodology (equal); Writing – original draft (equal). **Sergei Stepanoff:** Investigation (equal); Methodology (equal); Writing – review & editing (equal). **Aman Haque:** Conceptualization (equal); Formal analysis (equal); Funding acquisition (equal); Investigation (equal); Methodology (equal); Project administration (equal); Writing – review & editing (equal). **Douglas E. Wolfe:** Conceptualization (equal); Funding acquisition (equal); Supervision (equal); Writing – review & editing (equal). **Fan Ren:** Conceptualization (equal); Supervision (equal); Writing – review & editing (equal). **Stephen J. Pearton:** Conceptualization (equal); Project administration (equal); Supervision (equal); Writing – review & editing (equal).

DATA AVAILABILITY

The data that support the findings of this study are available within the article.

REFERENCES

[1] M. Meneghini, C. De Santi, I. Abid, M. Buffolo, M. Cioni, R. A. Khadar, L. Nela, N. Zagni, A. Chini, F. Medjdoub, G. Meneghesso, G. Verzellesi, E. Zanoni, and E. Matioli, J. Appl. Phys. **130**, 181101 (2021).
[2] L. Nela, M. Xiao, Y. Zhang, and E. Matioli, Appl. Phys. Lett. **120**, 190501 (2022).
[3] S. J. Pearton, A. Aitkaliyeva, M. Xian, F. Ren, A. Khachatrian, A. Ildefonso, Z. Islam, M. A. Jafar Rasel, A. Haque, A. Y. Polyakov, and J. Kim, ECS J. Solid State Sci. Technol. **10**, 055008 (2021).
[4] B. D. Weaver, T. J. Anderson, A. D. Koehler, J. D. Greenlee, J. K. Hite, D. I. Shahin, F. J. Kub, and K. D. Hobart, ECS J. Solid State Sci. Technol. **5**, Q208 (2016).
[5] S. J. Pearton, F. Ren, E. Patrick, M. E. Law, and A. Y. Polyakov, ECS J. Solid State Sci. Technol. **5**, Q35 (2016).
[6] O. Aktas, A. Kuliev, V. Kumar, R. Schwindt, S. Toshkov, D. Costescu, J. Stubbins, and I. Adesida, Solid-State Electron. **48**, 471 (2004).
[7] S. A. Vitusevich, A. M. Kurakin, R. V. Konakova, A. E. Belyaev, and N. Klein, Appl. Surf. Sci. **255**, 784 (2008).
[8] A. M. Kurakin, S. A. Vitusevich, S. V. Danylyuk, H. Hardtdegen, N. Klein, Z. Bougrioua, B. A. Danilchenko, R. V. Konakova, and A. E. Belyaev, J. Appl. Phys. **103**, 083707 (2008).
[9] Y. H. Hwang, Y. L. Hsieh, L. Lei, S. Li, F. Ren, S. J. Pearton, A. Yadav, C. Schwarz, M. Shatkhin, L. Wang, E. Flitsiyan, L. Chernyak, A. G. Baca, A. A. Allerman, C. A. Sanchez, and I. I. Kravchenko, J. Vac. Sci. Technol. B **32**, 031203 (2014).
[10] C. Sharma, A. K. Visvkarma, R. Laishram, A. Malik, K. Narang, S. Vinayak, and R. Singh, Semicond. Sci. Technol. **34**, 065024 (2019).
[11] M. P. Khanal, B. Ozden, K. Kim, S. Uprety, V. Mirkhani, K. Yapabandara, A. C. Ahyi, and M. Park, J. Vac. Sci. Technol. B **35**, 03D107 (2017).
[12] J. Lee, E. Flitsiyan, L. Chernyak, J. Salzman, and B. Meyler, ECS J. Solid State Sci. Technol. **6**, S3063 (2017).
[13] B. Luo, J. W. Johnson, F. Ren, K. K. Allums, C. R. Abernathy, S. J. Pearton, A. M. Dabiran, A. M. Wowchack, C. J. Polley, P. P. Chow, D. Schoenfeld, and A. G. Baca, Appl. Phys. Lett. **80**, 604 (2002).
[14] C. Schwarz, A. Yadav, M. Shatkhin, E. Flitsiyan, L. Chernyak, V. Kasiyan, L. Liu, Y. Y. Xi, F. Ren, S. J. Pearton, C. F. Lo, J. W. Johnson, and E. Danilova, Appl. Phys. Lett. **102**, 062102 (2013).
[15] A. Yadav, E. Flitsiyan, L. Chernyak, Y.-H. Hwang, Y.-L. Hsieh, L. Lei, F. Ren, S. J. Pearton, and I. Lubomirsky, Radiat. Eff. Defects Solids **170**, 377 (2015).
[16] G. Wenping, C. Chi, D. Huantao, H. Yue, Z. Jincheng, W. Chong, F. Qian, and M. Xiaohua, J. Semicond. **30**, 044002 (2009).
[17] S. Jha, E. V. Jelenković, M. M. Pejović, G. S. Ristić, M. Pejović, K. Y. Tong, C. Surya, I. Bello, and W. J. Zhang, Microelectron. Eng. **86**, 37 (2009).
[18] M. A. J. Rasel, S. P. Stepanoff, M. Wetherington, A. Haque, D. E. Wolfe, F. Ren, and S. Pearton, Appl. Phys. Lett. **120**, 124101 (2022).
[19] P. J. Martínez, E. Maset, P. Martín-Holgado, Y. Morilla, D. Gilabert, and E. Sanchis-Kilders, Materials **12**, 2760 (2019).
[20] H. Y. Kim, J. Kim, L. Liu, C. F. Lo, F. Ren, and S. J. Pearton, J. Vac. Sci. Technol. B **31**, 051210 (2013).
[21] F. Berthet, Y. Guhel, B. Boudart, H. Gualous, J. L. Trolet, M. Piccione, and C. Gaquière, Electron. Lett. **48**, 1078 (2012).
[22] S. A. Vitusevich, N. Klein, A. E. Belyaev, S. V. Danylyuk, M. V. Petrychuk, R. V. Konakova, A. M. Kurakin, A. E. Rengevich, A. Yu. Avksentyev, B. A. Danilchenko, V. Tilak, J. Smart, A. Vertiatchikh, and L. F. Eastman, Phys. Status Solidi A **195**, 101 (2003).
[23] T. Beechem, A. Christensen, D. S. Green, and S. Graham, J. Appl. Phys. **106**, 114509 (2009).
[24] S. Choi, E. Heller, D. Dorsey, R. Vetury, and S. Graham, J. Appl. Phys. **114**, 164501 (2013).
[25] B. S. Kang, S. Kim, J. Kim, F. Ren, K. Baik, S. J. Pearton, B. P. Gila, C. R. Abernathy, C.-C. Pan, G.-T. Chen, J.-I. Chyi, V. Chandrasekaran, M. Sheplak, T. Nishida, and S. N. G. Chu, Appl. Phys. Lett. **83**, 4845 (2003).
[26] C.-T. Chang, S.-K. Hsiao, E. Y. Chang, C.-Y. Lu, J.-C. Huang, and C.-T. Lee, IEEE Electron Device Lett. **30**, 213 (2009).
[27] K. Liu, H. Zhu, S. Feng, L. Shi, Y. Zhang, and C. Guo, Microelectron. Reliab. **55**, 886 (2015).
[28] M. Azize and T. Palacios, J. Appl. Phys. **108**, 023707 (2010).
[29] H. Zhu, X. Meng, X. Zheng, Y. Yang, S. Feng, Y. Zhang, and C. Guo, Solid-State Electron. **145**, 40 (2018).
[30] S. Choi, E. Heller, D. Dorsey, R. Vetury, and S. Graham, J. Appl. Phys. **113**, 093510 (2013).
[31] H. J. Park, C. Park, S. Yeo, S. W. Kang, M. Mastro, O. Kryliouk, and T. J. Anderson, Phys. Status Solidi C **2**, 2446 (2005).
[32] E. Cho, A. Mogilatenko, F. Brunner, E. Richter, and M. Weyers, J. Cryst. Growth **371**, 45 (2013).
[33] M. Chu, A. D. Koehler, A. Gupta, S. Parthasarathy, M. O. Baykan, S. E. Thompson, and T. Nishida, *Materials and Reliability Handbook for Semiconductor Optical and Electron Devices*, edited by O. Ueda and S. J. Pearton (Springer, New York, NY, 2013), pp. 381–429.
[34] J. A. del Alamo and J. Joh, Microelectron. Reliab. **49**, 1200 (2009).
[35] J. Joh, J. A. del Alamo, K. Langworthy, S. Xie, and T. Zheleva, Microelectron. Reliab. **51**, 201 (2011).
[36] N. M. Dang, W.-Y. Ku, Z.-Y. Wang, C.-H. Lin, T. Y.-F. Chen, and M.-T. Lin, Exp. Mech. **62**, 1489–1499 (2022).
[37] N. S. Al-Mamun, M. Wetherington, D. E. Wolfe, A. Haque, F. Ren, and S. Pearton, Microelectron. Eng. **262**, 111836 (2022).
[38] T. Kitamura, S. Nakashima, N. Nakamura, K. Furuta, and H. Okumura, Phys. Status Solidi C **5**, 1789 (2008).
[39] P. Cui, J. Mo, Y. Lv, C. Fu, H. Liu, A. Cheng, C. Luan, Y. Zhou, G. Dai, and Z. Lin, Sci. Rep. **8**, 12850 (2018).
[40] P. M. Bridger, Z. Z. Bandić, E. C. Piquette, and T. C. McGill, Appl. Phys. Lett. **74**, 3522 (1999).
[41] J. Zhao, Z. Lin, T. D. Corrigan, Z. Wang, Z. You, and Z. Wang, Appl. Phys. Lett. **91**, 173507 (2007).
[42] Y. J. Lv, X. B. Song, Y. G. Wang, Y. L. Fang, and Z. H. Feng, Nanoscale Res. Lett. **11**, 373 (2016).
[43] Y. Lv, Z. Lin, Y. Zhang, L. Meng, C. Luan, Z. Cao, H. Chen, and Z. Wang, Appl. Phys. Lett. **98**, 123512 (2011).
[44] S. Pradeep, R. Loganathan, S. Surender, K. Prabakaran, K. Asokan, and K. Baskar, Superlattices Microstruct. **120**, 40 (2018).
[45] T.-T. Luong, B. T. Tran, Y.-T. Ho, M.-T.-H. Ha, Y.-L. Hsiao, S.-C. Liu, Y.-S. Chiu, and E.-Y. Chang, Electron. Mater. Lett. **11**, 217 (2015).
[46] A. F. M. Anwar, R. T. Webster, and K. V. Smith, Appl. Phys. Lett. **88**, 203510 (2006).
[47] P. Cui, H. Liu, W. Lin, Z. Lin, A. Cheng, M. Yang, Y. Liu, C. Fu, Y. Lv, and C. Luan, IEEE Trans. Electron Devices **64**, 1038 (2017).